doi:10.3772/j.issn.1006-6748.2016.01.014

Selective transmission and channel estimation in massive MIMO systems①

Yang Ruizhe (杨睿哲)②[*,**], Zong Liang[**], Si Pengbo[*,**], Ma Dawei[**], Zhang Yanhua[*,**]
([*] Beijing Advanced Innovation Center for Future Internet Technology, Beijing University of Technology, Beijing 100124, P. R. China)
([**] College of Electronics Information and Control Engineering, Beijing University of Technology, Beijing 100124, P. R. China)

Abstract

Massive MIMO systems have got extraordinary spectral efficiency using a large number of base station antennas, but it is in the challenge of pilot contamination using the aligned pilots. To address this issue, a selective transmission is proposed using time-shifted pilots with cell grouping, where the strong interfering users in downlink transmission cells are temporally stopped during the pilots transmission in uplink cells. Based on the spatial characteristics of physical channel models, the strong interfering users are selected to minimize the inter-cell interference and the cell grouping is designed to have less temporally stopped users within a smaller area. Furthermore, a Kalman estimator is proposed to reduce the unexpected effect of residual interferences in channel estimation, which exploits both the spatial-time correlation of channels and the share of the interference information. The numerical results show that our scheme significantly improves the channel estimation accuracy and the data rates.

Key words: multiple-input multiple-output (MIMO), selective transmission, time-shifted pilots, Kalman

0 Introduction

Massive multiple-input multiple-output (MIMO) is a new breakthrough communication technique, which is based on the conventional MIMO features unprecedented numbers of service-antennas with a high ratio of service-antennas to terminals, channel state information derived from uplink pilots and time division duplex (TDD) reciprocity[1]. When MIMO arrays are made large, both opportunities and challenges[2] are met. The opportunities include increased capabilities of exploiting propagation channel, inexpensive low-power components built with the robustness to the interference. However, as one of the challenges, the effect of pilot contamination on massive MIMO appears to be much more profound than in classical MIMO, which results in a considerable channel estimation error by reusing pilots from one cell to another[3]. In addition, the favorable independent propagation that the Massive MIMO relies is not quite true. In reality, the MIMO channels are generally correlated because the large antenna arrays are not sufficiently well separated or the propagation environment does not offer rich enough scattering[4-6].

To tackle the challenge of the pilot contamination, effective channel estimations exploiting the channel characteristic are proposed[7,8]. In Ref. [7], an eigenvalue decomposition-based approach estimates the channel blindly from the received data just with a short training sequence to resolve the scalar ambiguity in the covariance matrix of the received signals. In Ref. [8], in the uplink training a rank-q channel approximation method based on compressive sensing is proposed. On the other hand, power control[9,10] and coordinated pilots assignment[11] are used to mitigate the pilot contamination. In the coordinated approach[11], users in different cells having the small channel correlations with each other are assigned to the same pilots, so that the pilot contamination is minimized. Different from the work in the traditional transmission with aligned pilots mentioned above, time-shifted pilots are proposed in Refs[12,13] to avoid pilots simultaneous transmission in adjacent cells, and it is possible to completely cancel the effect of interferences from the data to pilots on the assumption that the channels between the infinite antennas are independent. Later in Ref. [14], the performance improvement using time-shifted pilots under the effect of a finite number of antennas is confirmed. Also in the case of finite antennas, a zero-forc-

① Supported by the Program for Excellent Talents in Beijing (No. 2014000020124G040), National Natural Science Foundation of China (No. 61372089, 61571021) and National Natural Science Foundation of Beijing (No. 4132007, 4132015, 4132019).
② To whom correspondence should be addressed. E-mail: yangruizhe@bjut.edu.cn
Received on Mar. 9, 2015

ing transceiver is employed to resolve the interferences using time-shifted pilots Ref. [15]. However, as it is known that zero-forcing schemes eliminate the interference by orthogonalizing the channels, which brings loss of channel gains and is therefore inappropriate for the strong channel correlation environments.

In this study, the multicell massive multiuser MIMO using time-shifted pilots for the physical channels is investigated. Over these channels, the interferences become considerable for both the aligned pilots and time-shifted pilots transmissions. Here, the interferences in transmissions using time-shifted pilots is analyzed and a selective transmission is proposed, where parts of users are selected to temporarily stop downlink transmitting during a particular period. Using the proper selection, the strong interference from these selected users to the uplink pilots in adjacent cells is alleviated. Moreover, to improve the system performance under the residual interferences, a Kalman estimator is proposed to filer out both interferences and noise based on the time-spatial correlation of the channels and the share of the interference information.

1 System model

It is considered a network of L cells with full spectrum reuse. In each cell the base station with M antennas services K single-antenna users.

1.1 Physical channel model

Using the physical channel model, the channels in the t-th block (block-fading) from user k in the l-th cell to the base station (BS) in the l'-th cell can be represented as

$$\boldsymbol{h}_{l'kl}(t) = \frac{1}{\sqrt{P}}\sum_{p=1}^{P}\boldsymbol{\alpha}_{l'klp}(t)a(\theta_{l'klp}) \tag{1}$$

where the angular domain is divided into a large but finite number of directions P. Each direction is associated with a steering vector $\boldsymbol{a}(\theta_{l'klp})$ with the random angle-of-arrival (AOA) $\theta_{l'klp}$,

$$\boldsymbol{a}(\theta_{l'klp}) = [1, e^{-jf_1(\theta_{l'klp})}, \cdots, e^{-jf_{M-1}(\theta_{l'klp})}]^T \tag{2}$$

where $f_m(\theta_{l'klp}) = 2\pi\dfrac{mD}{\lambda}\cos(\theta_{l'klp})$, $m = 1, \cdots, M-1$, D is the antenna spacing at the BS and λ is the signal wavelength, such that $D \leqslant \lambda/2$. Note that $\theta_{l'klp}$ is uniformly distributed over $[\bar{\theta}_{l'kl} - \Delta\theta, \bar{\theta}_{l'kl} + \Delta\theta]$, and $\bar{\theta}_{l'kl} \in [0, 2\pi]$ is the mean AOA. It is considered that the propagation coefficient $\alpha_{l'klp}(t)$ is as zero mean complex Gaussian process of variance $\delta^2_{l'kl}$, following the Jakes' power spectrum of maximum Doppler frequency f_d.

Also using the physical channel model in Eq. (1), the channel $h_{k'l'kl}(t)$ is obtained from user k in the l-th cell to user k' in the l'-th cell during time block t, as shown in Fig. 1.

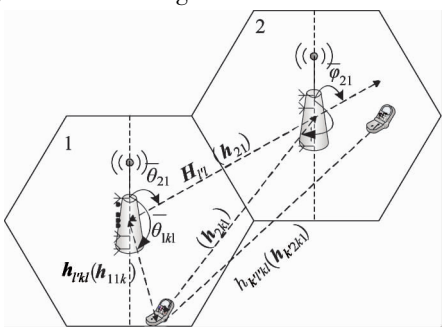

Fig. 1 Channels in the case of two cells

Let $\boldsymbol{H}_{l'l}$ denote the channel matrix between the BS in the l-th cell and the BS in the l'-th cell, which is assumed to be time invariant due to the fixed locations of the BSs[16].

$$\boldsymbol{H}_{l'l} = \frac{1}{\sqrt{P}}\sum_{p=1}^{P}\alpha_{l'lp}\boldsymbol{a}(\theta_{l'lp})\boldsymbol{b}^H(\varphi_{l'lp}) \tag{3}$$

where the propagation coefficient $\alpha_{l'lp}$ is as zero mean complex Gaussian random variable with variances $\delta^2_{l'l}$. The array steering vectors $\boldsymbol{a}(\theta_{l'lp})$ and $\boldsymbol{b}(\varphi_{l'lp})$ are

$$\begin{aligned}\boldsymbol{a}(\theta_{l'lp}) &= [1, e^{-jf_1(\theta_{l'lp})}, \cdots, e^{-jf_{M-1}(\theta_{l'lp})}]^T\\ \boldsymbol{b}(\varphi_{l'lp}) &= [1, e^{-jf_1(\varphi_{l'lp})}, \cdots, e^{-jf_{M-1}(\varphi_{l'lp})}]^T\end{aligned} \tag{4}$$

The random AOA $\theta_{l'lp}$, $\theta_{l'lp} \in [0, 2\pi]$ is uniformly distributed over $[\bar{\theta}_{l'l} - \Delta\theta, \bar{\theta}_{l'l} + \Delta\theta]$ with mean $\bar{\theta}_{l'l}$, and the angle-of-departure (AOD) $\varphi_{l'lp}$, $\varphi_{l'lp} \in [0, 2\pi]$ is uniformly distributed over $[\bar{\varphi}_{l'l} - \Delta\theta, \bar{\varphi}_{l'l} + \Delta\theta]$ with mean $\bar{\varphi}_{l'l}$.

1.2 Signals in the uplink and downlink

A TDD massive MIMO system is considered using time-shifted pilots, see Fig. 2. Assume that the uplink pilots of length τ are mutually orthogonal within a cell and therefore intra-cell interference is negligible in the channel estimation phase. The pilot sequence $\boldsymbol{s}_k = [s_{k1}\ s_{k2} \cdots s_{k\tau}]^T$ used by user k, $k = 1, 2, \cdots, K$, $|s_{k1}|^2 + \cdots + |s_{k\tau}|^2 = \tau$ is assumed.

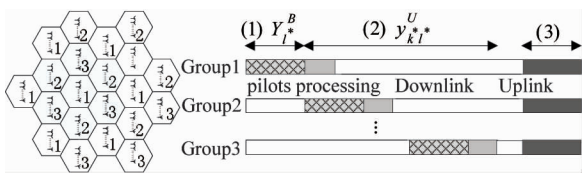

Fig. 2 Time-shifted pilot scheme with $G = 3$ groups

For simplicity, cell l^* in the 1st group is considered as the target cell, and the interference from the adjacent cells is only considered in this section, see

the gray area in Fig. 2, while other interferences will be explained in Section 2.3.

During the pilot phase, the $M \times \tau$ signal received at BS l^* is

$$\boldsymbol{Y}_{l^*}^{B} = \sum_{k=1}^{K} \sqrt{\rho_{kl^*}}\boldsymbol{h}_{l^*kl^*}\boldsymbol{s}_k^T + \sum_{k'=1}^{K}\sum_{l'\neq l^*}^{L} \underbrace{\sqrt{P_{k'l'}}\boldsymbol{H}_{l^*l'}\boldsymbol{w}_{k'l'}\boldsymbol{q}_{k'l'}^T}_{Interference} + N_0 \tag{5}$$

where ρ_{kl} is the transmit power from the k-th user in cell l to BS l, P_{kl} is the downlink power from BS l to its user k, $\boldsymbol{q}_{kl} = [q_{kl,1}, \cdots, q_{kl,\tau}]$ is the transmitted data vector in the downlink, w_{kl} is the beamforming and N_0 is the additive white noise with i. i. d, Gaussian distribution of zero mean and of variance $\sigma_{n_0}^2\boldsymbol{I}$. To simplify notation, time index t is omitted here.

In the downlink of both the 1st group and 3rd group when users in the 2nd group are sending pilot sequences, the received signal at user k^* in cell l^* can be written as

$$\begin{aligned} y_{k^*l^*}^{U} = {} & \sqrt{P_{k^*l^*}}\boldsymbol{h}_{l^*k^*l^*}^H\boldsymbol{w}_{k^*l^*}q_{k^*l^*} + v_{k^*l^*} \\ & + \sum_{\substack{k'=1,\\ k'\neq k^*}}^{K} \underbrace{\sqrt{P_{k'l^*}}\boldsymbol{h}_{l^*k^*l^*}^H\boldsymbol{w}_{k'l^*}q_{k'l^*}}_{Interference,I_1} \\ & + \sum_{k'=1}^{K}\sum_{l'\in G_2}^{L} \underbrace{\sqrt{\rho_{k'l'}}h_{k^*l^*k'l'}s_{k',i}}_{Interference,I_2} \\ & + \sum_{k'=1}^{K}\sum_{l'\in G_3}^{L} \underbrace{\sqrt{P_{k'l'}}\boldsymbol{h}_{l'k^*l^*}^H\boldsymbol{w}_{k'l'}q_{k'l'}}_{Interference,I_3} \end{aligned} \tag{6}$$

where I_1 is the intra-cell interference. I_2 and I_3 are pilots interference and data interference from the neighboring cells, respectively. The white Gaussian noise $v_{k^*l^*}$ is with zero mean and variance $\sigma_{n_0}^2$.

In the simultaneous uplink, BS applies signal processing with the receiving vector. Since the received signal in the uplink has similar formation to the downlink Eq. (6) but without I_2, on the downlink analysis is focused, and the extension to uplink can be straightforward.

2 User selection and channel estimation

2.1 Interference analysis

Here, relatively simple signal processing approaches are used that is maximal ratio combines (MRC) and transmission (MRT) for receiving and transmitting at the BS. The beamforming vector $\boldsymbol{w}_{kl}$ of user k is the normalized version of the estimated channel $\hat{\boldsymbol{h}}_{lkl}$:

$$\boldsymbol{w}_{kl} = \frac{\hat{\boldsymbol{h}}_{lkl}}{\|\hat{\boldsymbol{h}}_{lkl}\|} = \frac{\boldsymbol{h}_{lkl} + \boldsymbol{e}_{kl}}{\beta_{kl}\sqrt{M}}, \quad \hat{\boldsymbol{h}}_{lkl} = \boldsymbol{h}_{lkl} + \boldsymbol{e}_{kl} \tag{7}$$

where scalar $\beta_{kl} = \|\hat{\boldsymbol{h}}_{lkl}\| / \sqrt{M}$ is a normalization factor and $\boldsymbol{e}_{kl}$ is the channel estimation error.

Proposition 1 The effect of interferences depends on the positions of the interfering users and the interfered user in their respective serving cells and also the relative positions of these serving BSs. Specifically, the interact of these positions directly depends on the angles, including $\theta_{l^*kl^*p}\theta_{l'k'l'p'}$, $\varphi_{l^*l'p}$ and $\theta_{l^*l'p}$, as well as the variances of the propagation coefficients.

Proof: Using physical channel model, the interference in Eq. (5) can be derived as

$$\begin{aligned} & E\{\sqrt{P_{k'l'}}\boldsymbol{H}_{l^*l'}\boldsymbol{w}_{k'l'}\boldsymbol{q}_{k'l'}^T(\sqrt{P_{k'l'}}\boldsymbol{H}_{l^*l'}\boldsymbol{w}_{k'l'}\boldsymbol{q}_{k'l'}^T)^H\} \\ \overset{e_{k'l'}=0}{=} & \frac{\delta_{l^*l'}^2\delta_{l'k'l'}^2P_{k'l'}\tau}{\beta_{k'l'}^2MP^2}E\{\sum_{p=1}^{P}\begin{pmatrix}\boldsymbol{a}(\theta_{l^*l'p})\boldsymbol{b}^H(\varphi_{l^*l'p}) \\ \sum_{p'=1}^{P}\boldsymbol{a}(\theta_{l'k'l'p'})\boldsymbol{a}^H(\theta_{l'k'l'p'}) \\ \boldsymbol{b}(\varphi_{l^*l'p})\boldsymbol{a}^H(\theta_{l^*l'p})\end{pmatrix}\} \\ = & \frac{\delta_{l^*l'}^2\delta_{l'k'l'}^2P_{k'l'}\tau}{\beta_{k'l'}^2M}E\{\boldsymbol{a}(\theta_{l^*l'p})\boldsymbol{a}^H(\theta_{l^*l'p})\} \\ & \underbrace{E\{\boldsymbol{b}^H(\varphi_{l^*l'p})\boldsymbol{a}(\theta_{l'k'l'p'})\boldsymbol{a}^H(\theta_{l'k'l'p'})\boldsymbol{b}(\varphi_{l^*l'p})\}}_{I_{l^*k'l'}} \end{aligned} \tag{8}$$

with

$$\begin{aligned} I_{l^*k'l'} = {} & E\{\|\sum_{m=0}^{M-1}e^{-j2\pi m\frac{D}{\lambda}(\cos(\theta_{l'k'l'p'})-\cos(\varphi_{l^*l'p}))}\|^2\} \\ = {} & E\{\frac{1-\cos(2\pi M\frac{D}{\lambda}(\cos(\theta_{l'k'l'p'})-\cos(\varphi_{l^*l'p})))}{1-\cos(2\pi\frac{D}{\lambda}(\cos(\theta_{l'k'l'p'})-\cos(\varphi_{l^*l'p})))}\} \end{aligned} \tag{9}$$

which depends on $\bar{\theta}_{l'k'l'}$, $\bar{\varphi}_{l^*l}$ and $\Delta\theta$. Note that it is assumed $E\{\boldsymbol{q}_{kl}\boldsymbol{q}_{kl}^H\} = \tau\boldsymbol{I}$ and $\boldsymbol{e}_{k'l} = \boldsymbol{0}$, and the effect of $\boldsymbol{e}_{k'l} \neq \boldsymbol{0}$ will be discussed later. Therefore, the ratio of the interference to signal is approximated as

$$\begin{aligned} & \gamma_{kl^*k'l'}^{p} \\ = & \lim_{M\to\infty}\frac{E\{\sqrt{P_{k'l'}}\boldsymbol{H}_{l^*l'}\boldsymbol{w}_{k'l'}\boldsymbol{q}_{k'l'}^T(\sqrt{P_{k'l'}}\boldsymbol{H}_{l^*l'}\boldsymbol{w}_{k'l'}\boldsymbol{q}_{k'l'}^T)^H\}}{E\{\sqrt{\rho_{kl^*}}\boldsymbol{h}_{l^*kl^*}\boldsymbol{s}_k^T(\sqrt{\rho_{kl^*}}\boldsymbol{h}_{l^*kl^*}\boldsymbol{s}_k^T)^H\}} \\ = & \frac{\delta_{l^*l'}{}^2\delta_{l'k'l'}^2P_{k'l'}}{\beta_{k'l'}^2\rho_{kl^*}MP}\frac{E\{\boldsymbol{a}(\theta_{l^*l'p})\boldsymbol{a}^H(\theta_{l^*l'p})\}}{E\{\boldsymbol{a}(\theta_{l^*kl^*p})\boldsymbol{a}^H(\theta_{l^*kl^*p})\}}I_{l^*k'l'} \end{aligned} \tag{10}$$

The derivations in Eqs (8) ~ (10) show that the effect of interferences not only depends on the relationship between $\theta_{l^*kl^*p}$ and $\theta_{l^*l'p}$ in Eq. (10) but also the relationship between $\varphi_{l^*l'p}$ and $\theta_{l'k'l'p'}$ in $I_{l^*k'l'}$ Eq. (9). Thus, for the sensitive users who have the strong correlation between $\boldsymbol{a}(\theta_{l^*kl^*p})$ and $\boldsymbol{a}(\theta_{l^*l'p})$, a better way to deal with the interfering is to reduce the interferences from the strong interfering users, which can be defined by the expectation of $\cos(\theta_{l'k'l'p'}) - \cos(\varphi_{l^*l'p})$. Specifically, only when $|\theta_{l'k'l'p'} \pm \varphi_{l^*l'p}| > 0$, these inter-cell interference on the pilots can be minimized, which will be analyzed in Section 2.2.

In the case of $\boldsymbol{e}_{k'l'} \neq 0$, which is probably caused by the noise and interference in the pilots-based esti-

mation of $\boldsymbol{h}_{l'k'l'}$, see Eq. (5), $\boldsymbol{e}_{k'l'}$ is proportional to $\sum_{k''=1}^{K}\sum_{l''\neq l'}^{L}\boldsymbol{H}_{l'l''}\boldsymbol{w}_{k''l''}\boldsymbol{q}_{k''l''}^{T}+\boldsymbol{N}_0$. Consequently for the signal $\boldsymbol{Y}_{l^*}^{B}$, the interference is got caused by $\boldsymbol{e}_{k'l'}$ proportional to $\boldsymbol{H}_{l^*l'}(\sum_{k''=1}^{K}\sum_{l''\neq l'}^{L}\boldsymbol{H}_{l'l''}\boldsymbol{w}_{k''l''}\boldsymbol{q}_{k''l''}^{T}+N_0)\boldsymbol{q}_{kl^*}^{T}$. Obviously, the main parameters in this interference are in accordance with Proposition 1.

Proposition 2 The interference in the downlink transmission is mainly caused by the other downlinks both in the same cell and in adjacent cells. The effects of these interferences depend on the positions of both interfering users and interfered users, especially their AoAs, e.g., $\theta_{l^*k'l^*p}$ and $\theta_{l^*k^*l^*p'}$. Fortunately, the interferences from the uplink pilots in other cells are minor interferences when $\rho_{kl}\leqslant P_{kl}$ and even can be ignored.

Proof: Using physical channel model, interference I_1 in Eq. (6) can be written as

$$I_1=E\{\|\sqrt{P_{k'l^*}}\boldsymbol{h}_{l^*k^*l^*}^{H}\boldsymbol{w}_{k'l^*}q_{k'l^*}\|^2\}\overset{e_{k'l^*}=0}{=}\frac{\delta_{l^*k^*l^*}^2\delta_{l^*k'l^*}^2P_{k'l^*}}{\beta_{k'l^*}^2M}\underbrace{E\{\|\boldsymbol{a}^H(\theta_{l^*k^*l^*p})\boldsymbol{a}(\theta_{l^*k'l^*p'})\|^2\}}_{I'_{k'l^*}} \tag{11}$$

with

$$I'_{k'l^*}=E\{\frac{1-\cos(2\pi M\frac{D}{\lambda}(\cos(\theta_{l^*k'l^*p'})-\cos(\theta_{l^*k^*l^*p})))}{1-\cos(2\pi\frac{D}{\lambda}(\cos(\theta_{l^*k'l^*p'})-\cos(\theta_{l^*k^*l^*p})))}\} \tag{12}$$

which depends on $\bar{\theta}_{l^*k^*l^*}$, $\bar{\theta}_{l^*kl^*}$ and $\Delta\theta$. Furthermore, interference I_2 from the pilots is represented as

$$I_2=\|\sqrt{\rho_{k'l'}}h_{k^*l^*k'l'}s_{k',i}\|^2 \tag{13}$$

and interference I_3 is rewritten as

$$I_3=E\{\|\sqrt{P_{k'l'}}\boldsymbol{h}_{l'k^*l^*}^{H}\boldsymbol{w}_{k'l'}q_{k'l'}\|^2\}\overset{e_{k'l'}=0}{=}\frac{\delta_{l'k^*l^*}^2\delta_{l'k'l'}^2P_{k'l'}P}{\beta_{k'l'}^2M}\underbrace{E\{\|\boldsymbol{a}^H(\theta_{l'k^*l^*p})\boldsymbol{a}(\theta_{l'k'l'p'})\|^2\}}_{I'_3} \tag{14}$$

with

$$I'_3=E\{\frac{1-\cos(2\pi M\frac{D}{\lambda}(\cos(\theta_{l'k'l'p'})-\cos(\theta_{l'k^*l^*p})))}{1-\cos(2\pi\frac{D}{\lambda}(\cos(\theta_{l'k'l'p'})-\cos(\theta_{l'k^*l^*p})))}\} \tag{15}$$

which is determined by $\bar{\theta}_{l'k^*l^*}$, $\bar{\theta}_{l'k'l'}$ and $\Delta\theta$. Consequently, the asymptotic behavior of interference to signal $\lim_{M\to\infty}\frac{I_2}{MP_{k^*l^*}}=0$ is got, but $\lim_{M\to\infty}\frac{I_1}{MP_{k^*l^*}}$ and $\lim_{M\to\infty}\frac{I_3}{MP_{k^*l^*}}$ respectively depend on the specific AoAs of the users, where the power of received signal approaches $MP_{k^*l^*}$.

Considering $e_{kl}\neq 0$, similar to the proof in Proposition 1, e_{kl} is proportional to $\sum_{k''=1}^{K}\sum_{l''\neq l}^{L}\boldsymbol{H}_{ll''}\boldsymbol{w}_{k''l''}\boldsymbol{q}_{k''l''}^{T}+N_0$ and therefore the main parameters for $\sqrt{P_{k^*l^*}}\boldsymbol{h}_{l^*k^*l^*}^{H}\boldsymbol{e}_{k'l^*}\boldsymbol{q}_{k'l^*}^{T}$ in I_1 and $\sqrt{P_{k'l'}}\boldsymbol{h}_{l'k^*l^*}^{H}\boldsymbol{e}_{k'l'}\boldsymbol{q}_{k'l'}$ in I_3 are in accordance with Proposition 1.

2.2 Selective Transmission

Proposition 1 and Proposition 2 show that the problems of using time-shifted pilots are the interferences between pilots and data. Several approaches can mitigate interferences, including user selection and power allocation. Although the primary scenario of such studies is the traditional multiuser MIMO systems[17], the algorithms can be applied in this paper, where SINR can be obtained according to Section 3. However, these selections involve matrix operations of high computation complexity in large antenna array systems. Besides, the algorithms based on current channels cannot be directly used for the pilots transmission selection. Furthermore, even based on statistic spatial correlation, the traditional simple user reducing may lead to blind zone. Therefore, concentrating on the problems of users at the cell edge, we leave the effect of distance is left aside and a selective transmission of the strong interfering users is proposed based on AOA and AOD. Since the interference in Eq. (10) is large when $\cos(\theta_{l'k'l'p'})-\cos(\varphi_{l^*l'p})=0$ and gradually decreases with the difference $|\theta_{l'k'l'p'}\pm\varphi_{l^*l'p}|$ increasing, it can simply define user k to be the strong interfering user if

$$|\bar{\theta}_{l'k'l'}\pm\bar{\varphi}_{l^*l'}|\leqslant 2\tilde{\theta} \tag{16}$$

where $\tilde{\theta}$ is a controllable variable, satisfying $\tilde{\theta}=\min(\frac{\pi}{6},\Delta\theta)$. Using this definition, the strong interfering users in cell l with $\bar{\theta}_{l'k'l'}\leqslant\pm 2\tilde{\theta}\pm\bar{\varphi}_{l^*l'}$ are required to temperately stop their downlink transmitting when the pilots are transmitted in cell l^*. Note that the smaller angle spread $\Delta\theta$, the better is the performance of user selection using $\tilde{\theta}=\Delta\theta$, because the rate loss of the transmission stop is less than the throughput enhancement due to interference reduction. On the other hand, when $\Delta\theta$ is large, the number of stopped users is increasing. The tradeoff between the transmission stop and interference reduction should be further studied, and here a simple restriction $\tilde{\theta}\leqslant\frac{\pi}{6}$ is given to constraint the interfering users in cell l' for cell l^* to be stopped within two sectors. The algorithm of selective

transmission (see Fig. 4).

2.3 Cell grouping

In this section, the effect of interferences from the aspect of the whole systems is analyzed, which has been discussed individually in Section 2.2. Note that considering the effects of interferences in the system as a whole relate to the time assignment of the pilots and data in different cell groups. Therefore, cell grouping is one of the key issues.

For simplicity, the inter-group interference from adjacent cells is concentrated on but the interference from others are ignored, especially the cells relatively nearby in the same group. The problem of this intra-group interference is similar to that in the traditional aligned pilots scheme, which can be thought of as being analogous to frequency reuse that the more groups (larger G) the less intra-group interference. However, compared with inter-group interference, this intra-group interference is dramatically reduced when $G \geqslant 3$ due to larger distances between cells.

Considering the more severe inter-group interference from cell $l_{g'}$ (cell $l_{g'}$ belongs to group g') to cell l_g, using Eq. (16), it is found that users allocated around $\pm\varphi_{l_g l_{g'} q}$ in cell $l_{g'}$ are the main interference source and should be stopped, which are symmetrically distributed with respect to the antenna array. To have less temporally stopped users within a smaller area in cell $l_{g'}$, the cell l_g in group g should be allocated symmetrically with respect to the antenna array of BS $l_{g'}$ and the antenna array in each cell should be perpendicular to the cell edge (see Fig. 1 and Fig. 3).

Therefore, the selective transmissions during the time-shifted pilots respectively in the case of 3 cell groups and the case of 7 cell groups are shown in Fig. 3, where the users in the blue area are temporally stopped while the pilots are transmitted in gray areas.

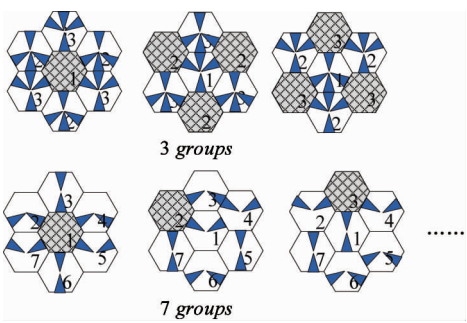

Fig. 3 Cell grouping and the selective transmission

2.4 Channel estimation

The proposed selective transmission strategy with cell grouping reduces the interference to a great extend, but there is still some residual interference, because of the unachievable asymptotic behavior of the interference and unfeasible infinite antenna arrays. This residual interference directly affects the channel estimation and system performance, see the analysis in Section 2.1. Therefore, efficient channel estimations resisting both the interference and noises are required. Obviously, the simplest LS estimation technique used in Ref. [13] is inapplicable. Using additional information like SNR and spatial feature, a covariance-based Bayesian estimation is proposed in Ref. [11]. Here, to fully explore the channel statistics, based on both the time coherence and spatial coherence of the channel, a channel estimation scheme using Kalman filter is proposed.

By vectorizing the received signal and noise, the signal received in Eq. (5) can be rewritten as

$$\begin{aligned}\boldsymbol{y}^B_{l^*}(t) &= \mathrm{vec}(\boldsymbol{Y}^B_{l^*}) = \sqrt{\rho_{k^*l^*}}\boldsymbol{S}_{k^*}\boldsymbol{h}_{l^*k^*l^*}(t) + \boldsymbol{n}'_0(t)\\ \boldsymbol{n}'_0(t) &= \sum_{l'\neq l^*}\sum_{k'\in U_{l'}} \mathrm{vec}\left(\sqrt{P_{k'l'}}\boldsymbol{H}_{l^*l'}\boldsymbol{w}_{k'l'}\boldsymbol{q}^T_{k'l'}(t)\right)\\ &\quad + \sum_{k''\in U_{l^*},k''\neq k}\sqrt{\rho_{k''l^*}}\boldsymbol{S}_{k''}\boldsymbol{h}_{l^*k''l^*}(t) + \mathrm{vec}(\boldsymbol{N}_0(t))\end{aligned} \tag{17}$$

where $\boldsymbol{S}_k = \boldsymbol{s}_k \otimes \boldsymbol{I}_M$, and $\boldsymbol{n}'_0(t)$ is the equivalent noise with the covariance given by

$$\begin{aligned}\sigma^2_{n'_0} &= E\{\boldsymbol{n}'_0(t)\boldsymbol{n}'_0(t)^H\} = \sigma^2_{n_0}\boldsymbol{I}_{M\tau}\\ &\quad + \sum_{l'\neq l^*}\sum_{k'\in U_l}\underbrace{P_{k'l'}\tau E\{\boldsymbol{I}_\tau \otimes (\boldsymbol{h}_{l^*l'}\boldsymbol{w}_{k'l'}(t)\boldsymbol{w}^H_{k'l'}(t)\boldsymbol{h}^H_{l^*l'})\}}_{R^I_{l^*,k',l'}}\\ &\quad + \sum_{k''\in U_1,k''\neq k}\underbrace{\rho_{k''l^*}E\{\boldsymbol{S}_{k''}\boldsymbol{h}_{l^*k''l^*}(t)\boldsymbol{h}^H_{l^*k''l^*}(t)\boldsymbol{S}^H_{k''}\}}_{R'^I_{l^*,k',l'}}\end{aligned} \tag{18}$$

where

$$\begin{aligned}\boldsymbol{R}^I_{l^*,k',l'} &= P_{k'l'}\tau\delta^2_{l^*l'}\boldsymbol{I}_\tau\\ &\quad \otimes \underbrace{\begin{pmatrix} E\{\boldsymbol{a}(\theta_{l^*l'p})\boldsymbol{a}^H(\theta_{l^*l'p})\}\\ \mathrm{Tr}\{\boldsymbol{w}_{k'l'}(t)\boldsymbol{w}^H_{k'l'}(t)E\{\boldsymbol{b}(\varphi_{l^*l'p})\boldsymbol{b}^H(\varphi_{l^*l'p})\}\}\end{pmatrix}}_{R^I_{l^*,k',l'}}\end{aligned} \tag{19}$$

Note that $\boldsymbol{R}'^I_{l^*,k',l'}$ can be ignored in Kalman recusion for the orthogonality. To obtain $\boldsymbol{R}^I_{l^*,k',l'}$ fortunately, before the pilots based estimation in cell l^*, the cells in other groups have the exactly the information of $\boldsymbol{w}_{k'l'}(t)\boldsymbol{w}^H_{k'l'}(t)$. For this reason, it is assumed that there is a coordination between the BSs to share $R^I_{l^*,k',l'}$, which produces little overhead but provides a better calculation of $\boldsymbol{R}^I_{l^*,k',l'}$.

Since the propagation coefficient $\alpha_{lklp}(t)$ follows the Jakes' power spectrum of maximum Doppler frequency f_d, the variations of $\boldsymbol{h}_{l^*k^*l^*}(t)$ can be well approached by an AR process of order one

$$\boldsymbol{h}_{l^*k^*l^*}(t) = \boldsymbol{A}\boldsymbol{h}_{l^*k^*l^*}(t-1) + \boldsymbol{\mu}(t) \tag{20}$$

where $\boldsymbol{\mu}(t)$ is the state noise with the covariance matrix

$\boldsymbol{\delta}_{\mu}^{2}$. Matrices $\boldsymbol{A}$ and $\boldsymbol{\delta}_{\mu}^{2}$ are obtained via the Yule-Walker equations:

$$\boldsymbol{A} = \boldsymbol{R}_{l*k*l*,0}\boldsymbol{R}_{l*k*l*,1}^{-1},$$
$$\boldsymbol{\delta}_{\mu}^{2} = \boldsymbol{R}_{l*k*l*,1} - \boldsymbol{A}\boldsymbol{R}_{l*k*l*,0}^{H} \quad (21)$$

with

$$\boldsymbol{R}_{l*k*l*,1} = E\{\boldsymbol{h}_{l*k*l*}(t)\boldsymbol{h}_{l*k*l*}(t-1)^{H}\} = \delta_{l*k*l*}^{2}R_{\tau}\boldsymbol{R}_{l*k*l*,0} \quad (22)$$

where $R_{\tau} = J_0(2\pi f_d T T_s)$ is the time coherence (T is the block length, T_s is the symbol duration, and $J_0(\cdot)$ is the zero order Bessel function of first kind). $\boldsymbol{R}_{l*k*l*,0} = E\{\boldsymbol{a}(\theta_{l*k*l*p})\boldsymbol{a}^{H}(\theta_{l*k*l*q})\}$ is the spatial coherence matrix, which can be obtained by $\bar{\theta}_{l*k*l*}$ and $\Delta\theta$[4].

The state model Eq. (20) and the observation model Eq. (17) allow us to use Kalman filter to track the channels through two stages:

Time update equations:

$$\boldsymbol{\varepsilon}'(t) = \boldsymbol{A}\boldsymbol{\varepsilon}(t-1)\boldsymbol{A}^{H} + \boldsymbol{\delta}_{\mu}^{2},\ \hat{\boldsymbol{h}}'_{l*k*l*}(t-1) = \boldsymbol{A}\hat{\boldsymbol{h}}_{l*k*l*}(t-1)$$

Measurement update equations:

$$\boldsymbol{K}(t) = \boldsymbol{\varepsilon}'(t)\boldsymbol{S}_{k*}^{H}[\boldsymbol{S}_{k*}\boldsymbol{\varepsilon}'(t)\boldsymbol{S}_{k*}^{H} + \sigma_{n_0}^{2}]^{-1}$$
$$\boldsymbol{\varepsilon}(t) = [\boldsymbol{I}_M - \boldsymbol{K}(t)\boldsymbol{S}_{k*}]\boldsymbol{\varepsilon}'(t)$$
$$\hat{\boldsymbol{h}}_{l*k*l*}(t) = \hat{\boldsymbol{h}}'_{l*k*l*}(t-1) + \boldsymbol{K}(t)[\boldsymbol{y}_{l*}^{B}(t) - \boldsymbol{S}_{k}\hat{\boldsymbol{h}}'_{l*k*l*}(t-1)]$$

where $\boldsymbol{\varepsilon}'(t)$, $\boldsymbol{\varepsilon}(t)$ are the a priori and the a posteriori error estimate covariance matrix, $\boldsymbol{K}(t)$ is the Kalman gain and $\hat{\boldsymbol{h}}_{l*k*l*}(t)$ is the estimated channel result. Also $\hat{\boldsymbol{h}}_{l*k*l*}(0) = \boldsymbol{0}_{M\times 1}$, $\boldsymbol{\varepsilon}(t) = \delta_{l*k*l*}^{2}\boldsymbol{R}_{l*k*l*,0}$ are initiated.

Block $= 1,2,\ldots,\infty$
For $g = 1,\ldots,G$
BS $l_{g'}$ stops downlink transmit of user k''
BS $l_{g'}$ keeps downlink transmit of user k'
users $\forall k \in \boldsymbol{U}_{l_g}$ transmit pilots
BS l_g estimates channels under interferences from $\boldsymbol{U}_{l_{g'}} = \{k'\}$
BS l_g shares $R^{I}_{l_{g'},k',l_g}$
if (*Block* $= 1$)
$\{k'',k' \mid g' < g, \|\bar{\theta}_{l_g,k''l_g} \pm \bar{\varphi}_{l_g l_{g'}}| \le 2\tilde{\theta}, |\bar{\theta}_{l_g,k'l_g} \pm \bar{\varphi}_{l_g l_{g'}}| \ge 2\tilde{\theta}\}$
else
$\{k'',k' \mid g' \ne g, \|\bar{\theta}_{l_g,k''l_g} \pm \bar{\varphi}_{l_g l_{g'}}| \le 2\tilde{\theta}, |\bar{\theta}_{l_g,k'l_g} \pm \bar{\varphi}_{l_g l_{g'}}| \ge 2\tilde{\theta}\}$
end
End

Fig. 4 Description of the proposed scheme

3 Simulation results

A symmetric multicell network that adopts the model of a cluster of hexagonally shaped cells[6] is proposed. Some basic simulation parameters are given: cell radius 1km, number of user per-cell 10, path loss exponent $\gamma = 3$, Carrier frequency 2GHz, pilot length 10 and Number of paths $P = M$, block length $T = 100$ and Doppler spread $f_d T T_s = 0.1$. The AOAs have uniform distributions with the angle spreads $\Delta\theta = 20$ degrees of all channels. It is assumed that users uniformly distributed on the cell edge $d_0 = 800$m have $\delta_{lkl}^{2} = 1$ to its serving BS and accordingly, the variance of other propagation coefficients can be obtained using the geographical distance d.

The proposed scheme (Proposed) is evaluated with 3 cell groups (Proposed (3)) and 7 cell groups (Proposed (7)), respectively. In addition, the performance of the proposed selective transmission using time-shifted pilots and cell grouping but Bayesian estimator (STSP- Bayesian estimation), the generall transmission using time-shifted pilots[13] and Kalman estimation (TSP-Kalman estimation), the transmissions employing aligned pilots (Aligned pilots) and coordinated assignment of aligned pilots (Coordinated aligned pilots)[11] is presented.

Fig. 5, Fig. 6, Fig. 7 and Fig. 8 give the performance versus number of antennas at BS with the downlink SNR 12dB and uplink SNR 7dB. Fig. 5 shows that both the proposed selective transmission and the coordinated aligned pilots have lower estimation errors than the traditional transmissions using aligned pilots and time-shifted pilots, because of the interference reduction by exploiting the special correlation. Besides, the estimators also play an important role in estimation accuracy that the proposed scheme performs better than STSP-Bayesian estimation. Therefore, the proposed scheme has much more flexibility and provides the lowest estimation error by both the selective interference reduction and effective filtering of interferences based

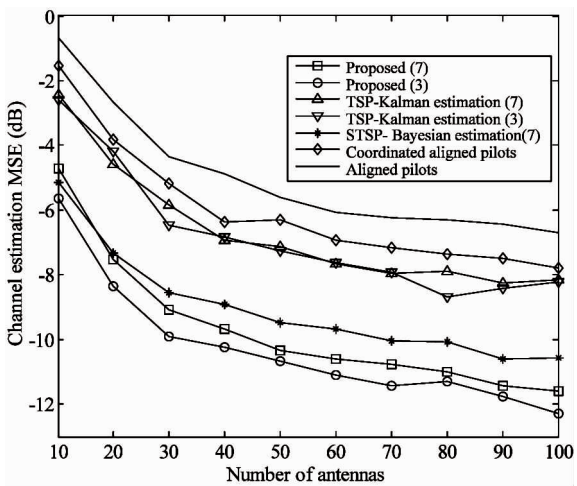

Fig. 5 Channel Estimation MSE vs. BS antenna number

on the time-spacial correlation. Since the correlation is increasing with the increased antennas, the proposed scheme improves quickly with antennas from 10 to 40.

Fig. 6 shows the average received downlink SINR at user versus the antennas increasing. Obviously, the proposed selective transmissions have higher SINR, because of interference reductions from the stopped strong interfering users. Also the estimation error plays an important role, and therefore the proposed scheme shows better SINR. Moreover, the proposed scheme with 7 cell groups has higher average SINR than the case of 3 cell groups due to long time of stopping users and pilots transmission in adjacent cells.

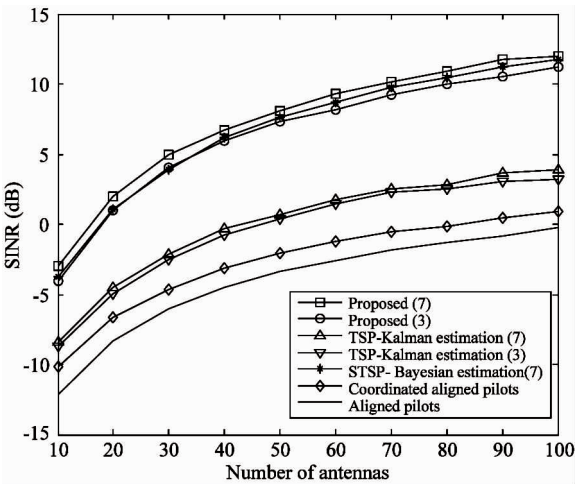

Fig. 6 Downlink SINR vs. BS antenna number

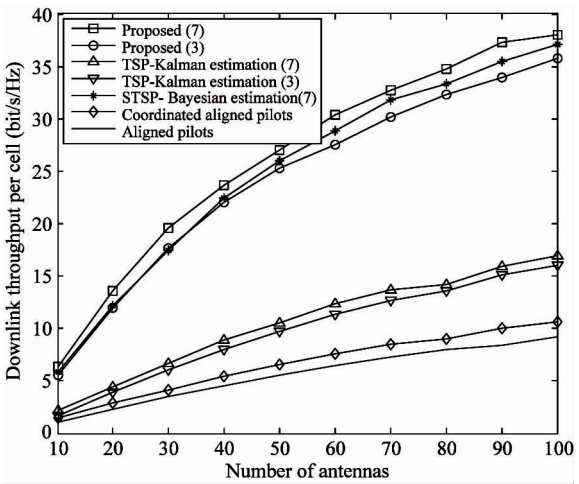

Fig. 7 Downlink system throughput vs. BS antenna number

Fig. 7 and Fig. 8 show the downlink and uplink throughput per cell versus antennas increasing, respectively. The proposed scheme has the higher throughput both in the downlink and uplink due to the interference reducing the filtering, which provides improvement over the loss of the user stop when the antenna size is large. In the comparison between the proposed schemes of 3 cells groups and of 7 cell groups, the 7 cell groups have higher downlink throughput for average downlink SINR but lower uplink throughput for a bit poorer channel estimation.

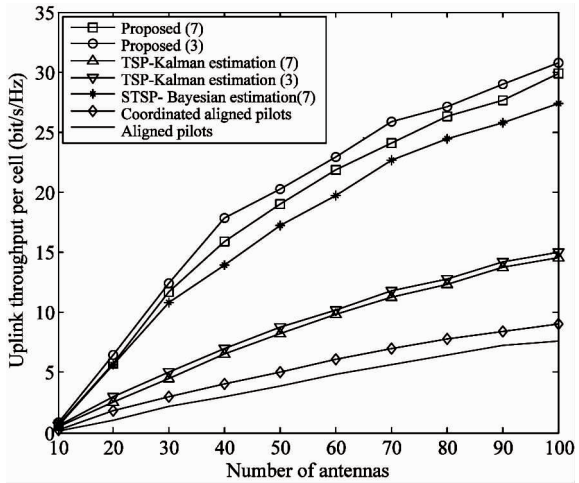

Fig. 8 Uplink system throughput vs. BS antenna number

Fig. 9 gives the channel MSE versus uplink SNR with downlink SNR 12dB and M = 50 antennas at the BS. Both the proposed schemes and the aligned pilots transmission have little estimation MSE improvement with the SNR from 10dB to 30dB. It demonstrates that the interference is the main factor affecting estimation errors and thus the increase of power cannot provides significant improvements. For this reason, the proposed scheme gets a better performance by effectively reducing interference.

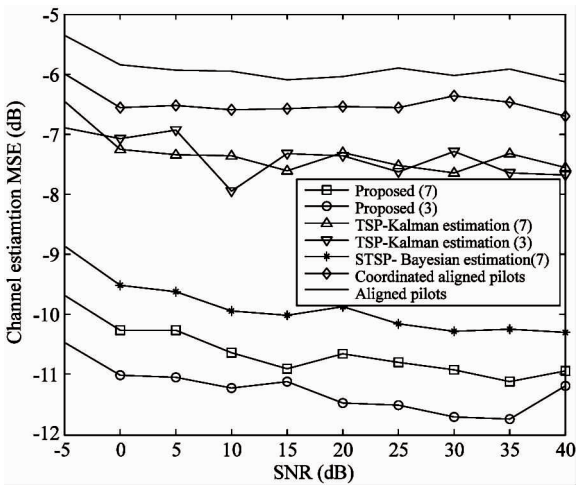

Fig. 9 Channel Estimation MSE vs. SNR

4 Conclusions

A scheme of selective transmission using time-shifted pilots with cell grouping is proposed. Based on physical channel models, the behavior of interfering is analyzed. It shows that except for the intra-cell interferences, inter-cell interferences between the pilots and data become the challenges. To cope with these problems, the interference by selecting users to temporally stop transmitting and minimize the stopped users by cell grouping design is reduced. Further, to deal with the inevitably residual interference, the channel estimation using Kalman tracking to filer out both the interference and noise is proposed. The numerical results show that both the proposed transmission and estimation play important roles in the improvement of system performance.

References

[1] Hoydis J, Hosseini K, Brink S t, et al. Making smart use of excess antennas: massive MIMO, small cells, and TDD. *Bell Labs Technical Journal*, 2013, 18(2): 5-21

[2] Rusek F, Persson D, Lau B K, et al. Scaling up MIMO: opportunities and challenges with very large arrays. *IEEE Signal Process*, 2013, 30(1): 40-60

[3] Jose J, Ashikhmin A, Marzetta T L, et al. Pilot contamination and precoding in multi-cell TDD systems. *IEEE Trans Wireless Commun*, 2011, 10(8): 2640-2651

[4] Tsai J A, Buehrer R M, Woerner B D. The impact of AOA energy distribution on the spatial fading correlation of linear antenna array. In: Proceedings of the IEEE Vehicular Technology Conference, Birmingham, UK, 2002. 933-937

[5] Ngo H Q, Marzetta T L, Larsson E G. Analysis of the pilot contamination effect in very large multicell multiuser MIMO systems for physical channel models. In: Proceedings of the IEEE International Conference on Acoustics, Speech and Signal Processing (ICASSP), Prague, Czech Republic, 2011. 3464-3467

[6] Hoydis J, Brink S t, Debbah M. Massive MIMO in the UL/DL of cellular networks: how many antennas do we need. *IEEE J Sel Areas Commun*, 2013, 31(2): 160-171

[7] Ngo H Q, Larsson E G. EVD-based channel estimation in multicell multiuser MIMO systems with very large antenna arrays. In: Proceedings of the IEEE International Conference on Acoustics, Speed and Signal Processing (ICASSP), Kyoto, Japan, 2012. 3249-3252

[8] Nguyen S, Ghrayeb A. Compressive sensing-based channel estimation for massive multiuser MIMO systems. In: Proceedings of the IEEE Wireless Communications and Networking Conference (WCNC), Shanghai, China, 2013. 2890-2895

[9] Cottatellucci L, Muller R R, Vehkapera M. Analysis of pilot decontamination based on power control. In: Proceedings of the IEEE Vehicular Technology Conference (VTC), Dresden, Germany, 2013. 1-5

[10] Muller R R, Vehkapera M, Cottatellucci L. Blind pilot decontamination. *IEEE Journal of Selected Topics in Signal Processing*, 2013, 8(5): 773-786

[11] Yin H, Gesbert D, Filippou M, et al. A coordinated approach to channel estimation in large-scale multiple-antenna systems. *IEEE Journal on Selected Areas in Communications*, 2013, 31(2): 264-273

[12] Appaiah K, Ashikhmin A, Marzetta T L. Pilot Contamination Reduction in Multi-User TDD Systems. In: Proceedings of the 2010 IEEE International Conference on Communications (ICC), Cape Town, South Africa, 2010. 1-5

[13] Fernandes F, Ashikhmin A, Marzetta T L. Inter-cell interference in noncooperative TDD large scale antenna systems. *IEEE Journal on Selected Areas in Communications*, 2013, 31(2): 192-201

[14] Mahyiddin W A W M, Martin P A, Smith P J. Pilot Contamination Reduction Using Time-Shifted Pilots in Finite Massive MIMO Systems. In: Vehicular Technology Conference (VTC Fall), Vancouver, Canada, 2014. 1-5

[15] Shi J, Xiaoyu W, Zheng L, et al. Zero-forcing beamforming in massive MIMO systems with time-shifted pilots. In: Proceedings of the 2014 IEEE International Conference on Communications (ICC), Sydney, Australia, 2014. 4801-4806

[16] Sayeed A M. Deconstructing Multiantenna Fading Channels. *IEEE Transactions on Signal Processing*, 2002, 50(10): 2563-2579

[17] Zukang S, Runhua C, Andrews J G, et al. Low complexity user selection algorithms for multiuser MIMO systems with block diagonalization. *IEEE Transactions on Signal Processing*, 2006, 54(9): 3658-3663

Yang Ruizhe, born in 1982. She received the Ph. D. degree in Signal and Information Processing from Beijing University of Posts and Telecommunications, Beijing, P. R. China, in 2009. Since 2009, she has been with the School of Electronic Information and Control Engineering, Beijing University of Technology, Beijing, P. R. China. Her current research interests are wireless communications, including the resource allocation in OFDM systems, MIMO systems, and the channel estimation.